MOLECULAR AND CELLULAR BIOLOGY, Apr. 1996, p. 1794–1804 Vol. 16, No. 4
0270-7306/96/$04.00+0

Expression and Activity of L-Myc in Normal Mouse Development

KIMI S. HATTON,[1,2] KATHLEEN MAHON,[3] LYNDA CHIN,[1,4] FUNG-CHOW CHIU,[5] HAN-WOONG LEE,[1] DAMIN PENG,[5] SHARON D. MORGENBESSER,[1] JAMES HORNER,[1] AND RONALD A. DEPINHO[1]*

Departments of Microbiology and Immunology and of Medicine,[1] Division of Dermatology,[4] and Department of Neurology,[5] Albert Einstein College of Medicine, Bronx, New York 10461; Department of Biochemistry and Fels Institute of Cancer Research and Molecular Biology, Temple University School of Medicine, Philadelphia, Pennsylvania 19140[2]; and Laboratory of Mammalian Genes and Development, National Institute of Child Health and Human Development, National Institutes of Health, Bethesda, Maryland 20892[3]

Received 18 September 1995/Returned for modification 15 November 1995/Accepted 17 January 1996

To determine the role of L-Myc in normal mammalian development and its functional relationship to other members of the Myc family, we determined the normal patterns of L-*myc* gene expression in the developing mouse by RNA in situ hybridization and assessed the phenotypic impact of L-Myc deficiency produced through standard gene targeting methodology. L-*myc* transcripts were detected in the developing kidney and lung as well as in both the proliferative and the differentiative zones of the brain and neural tube. Despite significant expression of L-*myc* in developing mouse tissues, homozygous null L-*myc* mice were found to be viable, reproductively competent, and represented in expected frequencies from heterozygous matings. A detailed histological survey of embryonic and adult tissues, characterization of an embryonic neuronal marker, and measurement of cellular proliferation in situ did not reveal any congenital abnormalities. The lack of an apparent phenotype associated with L-Myc deficiency indicates that L-Myc is dispensable for gross morphological development and argues against a unique role for L-Myc in early central nervous system development as had been previously suggested. Although overlapping expression patterns among *myc* family members raise the possibility of complementation of L-Myc deficiency by other Myc oncoproteins, compensatory changes in the levels of c- and/or N-*myc* transcripts were not detected in homozygous null L-*myc* mice.

Targeted gene inactivation in the mouse affords a direct experimental means of addressing whether highly related members of a multigene family have unique or overlapping roles. Such a strategy has been utilized with the goal of delineating the functions of each member of the Myc family in the developing mouse (14, 16, 58, 66; also the present report). The *myc* family of cellular oncogenes encodes three structurally and functionally related members, c-Myc, N-Myc, and L-Myc, that are believed to play key roles in the regulation of cellular proliferation, differentiation, and apoptosis (19, 22, 38). Although their precise mechanism of action remains to be fully elucidated, current evidence supports the view that Myc oncoproteins function as sequence-specific transcription factors governing the regulation of target genes integral to these processes (for reviews, see reference 68 and references therein).

The c-*myc* gene was first identified as the cellular homolog of an avian retrovirus transforming gene, v-*myc* (64, 65). Identification of the N-*myc* gene was made possible on the basis of its homology to c-*myc* and its amplification in human neuroblastomas (18, 32, 33, 62). Similarly, L-*myc* was identified as a *myc*-related sequence amplified in a subset of human small-cell lung carcinomas (30, 50) and then independently isolated from normal murine and human genomes on the basis of homology to N-*myc* (17, 36). Members of the Myc family share features in their gene and protein structures, including (i) a three-exon gene organization that gives rise to short-lived transcripts with large 5′ and 3′ untranslated regions and (ii) nucleus-localized, related gene products with the capacity to bind DNA in a sequence-specific manner (10, 53), transactivate gene expression in vitro (2, 5, 12, 28), and oligomerize with another basic region-helix-loop-helix–leucine zipper (bHLH/LZ) protein, Max (1, 6, 11, 29, 49, 52, 71). On the biological level, all three *myc* family genes can cooperate with a mutant H-*RAS* gene to transform early-passage rat embryo fibroblasts (17, 35, 63, 73) and can generate tumors when overexpressed in transgenic mice (for a review, see reference 43). The use of dominant-negative mutant forms of Myc has revealed that members of the Myc family function through common genetic pathways to transform cells (49).

Several lines of evidence support the view that the members of the *myc* family have separable physiological functions, including (i) their conservation as distinct genes over a large phylogenetic distance from zebra fish to humans (reference 60 and references therein; 61), (ii) their dispersed chromosomal locations (reviewed in reference 44), and (iii) marked differences in their oncogenic and transactivation potencies, with c-Myc possessing strong activity and N- and L-Myc exhibiting moderate and weak transforming and transactivation potential, respectively (4, 9, 17, 49, 72). Support for their unique and essential roles in development also stems from their distinct patterns of expression with respect to cell type and developmental stage; however, extensive overlap in *myc* family gene expression does exist (for a review, see reference 19).

During development, expression of c-, N-, and L-*myc* is at its highest levels during embryonic stages and is downregulated as mature organ systems become growth arrested and terminally differentiate postnatally. Although transcripts of all three genes are detectable in preimplantation embryos (24a), with the onset of gastrulation, the N-*myc* gene is abundantly expressed in embryonic cells while c-*myc* transcripts predominate

* Corresponding author. Mailing address: Department of Microbiology and Immunology, Albert Einstein College of Medicine, 1300 Morris Park Ave., Bronx, NY 10461. Phone: (718) 430-2822. Fax: (718) 430-8972. Electronic mail address: depinho@aecom.yu.edu.

in extraembryonic tissues (21). As development progresses through midgestation, the distribution of N-*myc* transcripts becomes restricted to particular organs (such as the brain and kidney) while that of c-*myc* is more broad (21, 47, 59). Notably, L-*myc* has a more limited tissue distribution than other *myc* family genes and appears to be coexpressed with c- and/or N-*myc* (74). During midgestation, high-level c-*myc* expression correlates well with active cellular proliferation, whereas strong N- and L-*myc* expression is also found in postmitotic cells that are undergoing differentiation. These expression profiles have fueled speculation that c-Myc plays a role in cellular proliferation whereas N- and L-Myc are more closely linked to processes of differentiation (43, 47, 48), a hypothesis that has been supported by gain-of-function studies performed with transgenic mice (44).

Homozygous null c-*myc* and N-*myc* mice die on embryonic days 10 and 12 (E10 and E12), respectively. Mice devoid of N-Myc exhibit a marked delay in development as well as a decrease in size and diminished cellularity of organs that normally express abundant levels of N-*myc* mRNA during their development (14, 58, 66); in particular, the cranial and spinal ganglia, mesonephros, lung, and gut were most severely affected (14, 58, 66). Abnormalities appear despite compensatory up-regulation of c-*myc* in the neuroepithelium (66), a tissue that normally expresses N-*myc*, a finding suggesting a unique and essential role for N-Myc at this stage in development. Similarly, although N-*myc* expression is strong in many cell types during early gestation, this does not rescue the homozygous null c-*myc* condition, whose embryonic lethality is associated with a marked reduction in embryo size and a generalized delay in the early development of multiple organs, including the heart, the pericardium, and the neural tube, potentially due to a defect in vascularization (16). Perhaps the most unexpected result of the c- and N-*myc* studies was the survival of these mutant embryos to developmental stages well beyond the onset of abundant c- and N-*myc* expression. Redundant functional properties among members of the Myc family during early, but not later, embryonic development could provide a potential explanation for the survival of mutant embryos through early embryonic stages (14, 16, 58, 66). Indeed, molecular complementation appears to be the case, as embryos null for *max*, the obligate partner of all three Myc oncoproteins, become arrested much earlier in development than null c- or N-*myc* embryos (35a).

In this study, we have examined L-*myc* gene expression during normal mouse development and used gene targeting methodology to produce a loss-of-function mutation in the L-*myc* gene with the goal of determining the developmental role of L-Myc and its functional relationship to other members of the Myc family. RNA in situ hybridization studies show that L-*myc* is expressed throughout the developing central nervous system with the highest levels detected in the neuroectoderm of the brain and neural tube. Despite this expression and the postulated role of L-*myc* as a pivotal developmental regulator of neuronal differentiation, homozygous null L-*myc* mice are healthy and indistinguishable from their wild-type littermates. The functional implications of L-Myc's dispensability are discussed.

MATERIALS AND METHODS

Detection of embryonic expression of L-myc by in situ hybridization. Embryos were fixed in 4% paraformaldehyde in phosphate-buffered saline (PBS) and embedded in paraffin. Sections (3 to 4 μm thick) were cut and affixed to poly-L-lysine-coated slides. Sense and antisense ^{35}S-labeled riboprobes were generated from appropriately linearized plasmids by in vitro transcription with T3 and T7 RNA polymerases (Stratagene) and ^{35}S-UTP under standard conditions. The L-*myc* probe (pTL180.72) contained a 180-bp *Pst*I fragment derived from untranslated sequences in exon 3 cloned into the vector pT7T3 19U. The N-*myc* probe (pMN1.2) was a 540-bp *Cla*I-*Pst*I fragment from the third exon of N-*myc* cloned into pSP65. The c-*myc* probe (pKSc370) was a 370-bp *Pvu*II-*Xho*I fragment from the third exon cloned into pBluescript. Slide pretreatment and in situ hybridization were performed as previously described (40). The slides were exposed to Kodak NTB-2 emulsion and developed after 14 to 30 days.

Cell culture and electroporation of ES cells. Mouse embryonal stem (ES) cells were maintained as previously described (55) and cultured in Dulbecco's modified Eagle's medium supplemented with 15% fetal calf serum (Sigma) and 1,000 U of leukemia inhibitory factor per ml on γ-irradiated SNL feeder layers (a kind gift from Allan Bradley). The mouse ES cell line used was E14a, derived by Martin Hooper (24) and provided by Raju Kucherlapati. Details regarding the design of the L-*myc* targeting construct are described in the legend to Fig. 3. For electroporation, 5×10^7 cells were trypsinized, washed in PBS, resuspended in 0.8 ml of PBS containing 10 to 25 μg of linearized L-*myc*/Neo/Tk vector (see Fig. 3A), and incubated on ice for 5 to 10 min. Electroporation was performed in a 0.4-cm-diameter cuvette by using a Bio-Rad gene pulser at 250 mV and 500 μF. Following a 10-min incubation at room temperature, electroporated ES cells were plated onto 10 6-cm-diameter tissue culture plates containing the medium described above. Thirty-six to 50 h later, two plates received G418 (0.125 mg/ml; active ingredient); the remaining eight plates received both G418 (0.125 mg/ml; active ingredient) and ganciclovir (2 μM [final concentration]). On day 5 of selection, the G418 dose was increased to 0.15 mg/ml (active), and selection was continued for an additional 4 to 5 days. On days 9 and 10 of selection, individual clones were picked, dispersed into a single cell suspension in 0.25% trypsin–1 mM EDTA, and seeded into two wells, each in a separate 48-well tissue culture plate. After 5 to 7 days, one plate was used for DNA isolation for Southern analysis by standard protocols. The ES cultures in the duplicate plate were frozen by slow cooling to −80°C following replacement of ES culture medium with 200 μl of ice-cold DMEM containing 10% FCS and 10% dimethyl sulfoxide.

Blastocyst injections. Approximately 10 to 15 ES cells carrying one null allele of the mouse L-*myc* gene were microinjected into C57BL/6 blastocysts; five to seven microinjected embryos were transferred into each uterine horn of a CD1 pseudopregnant female at 2.5 days postcoitum. The degree of chimerism was determined by agouti coat color contribution.

Analysis of DNA and RNA. To distinguish between wild-type and targeted L-*myc* alleles, Southern blots containing *Bam*HI-digested genomic DNA derived from 1 well of a 48-well plate were assayed for hybridization with a radiolabeled 800-bp *Eco*RI fragment containing 5′ flanking L-*myc* genomic sequences located beyond the 5′ end of the L-*myc*/Neo/Tk vector. For Northern (RNA) blot studies, total cellular RNA derived from staged whole mouse embryos and from newborn mouse tissues was isolated by the LiCl method as described previously (3). Embryos were staged as 0.5 days at noon of the day on which the vaginal plug was found. Twenty micrograms of total RNA was used in each lane and was judged to be intact and evenly loaded by ethidium bromide staining and by hybridization with the rat glyceraldehyde-3-phosphate dehydrogenase (GAPDH) gene (69). Following hybridization with c-, N-, or L-*myc*-specific probes, the same filter was assayed for hybridization with GAPDH as a control for sample loading. To compare *myc* family gene expression between wild-type and null L-*myc* samples, quantitation of hybridization signals was performed with the aid of the Molecular Dynamics model 300 series computing densitometer program Imagequant. Probes used for Northern blot studies included the following: (i) for c-*myc*, a 780-bp *Pst*I-*Xho*I coding domain fragment derived from pMc-*myc*54 (67) (a gift from Ken Marcu); (ii) for N-*myc*, a 560-bp *Cla*I-*Pst*I exon 3 fragment isolated from pN77 (18); and (iii) for L-*myc*, a 560-bp *Bam*HI-*Hin*dIII exon 3 fragment isolated from B1 (36).

Histological analysis, bromodeoxyuridine (BrdU) assays, and indirect immunoperoxidase staining. Staged whole embryos or 2-month-old adult organs were fixed in 10% buffered formalin (Polyscientific) overnight, dehydrated through a graded ethanol series, cleared in xylene, and embedded in Paraplast Xtra (VWR). Microtome sections (5 μm thick) were affixed to poly-L-lysine-coated microslides, deparaffinized, rehydrated, and blocked with normal goat serum (Vector Laboratories). Neuronal development was evaluated by immunocytochemical staining of paraffin sections with an antiserum raised specifically against a 66-kDa neurofilament protein, NF-66, that is abundantly expressed in both embryonic and postnatal brain neurons. NF-66 and the polyclonal rabbit antiserum were described elsewhere (15). Primary incubations were carried out with antiserum at a 1:1,000 dilution for 2 h at room temperature in 5% bovine serum albumin-PBS. The secondary incubations were carried out with biotinylated anti-rabbit serum (Vector Laboratories) at a 1:200 dilution for 1 h at room temperature and were followed by avidin and peroxidase-conjugated biotin detection (Vector Laboratories). The analysis of cellular proliferation (progression through S phase) of 15.5-day-old embryos was performed as described elsewhere (44).

Antibody preparation and Western immunoblot analysis. A mouse L-Myc-specific carboxy-terminal peptide (CRQQQLQKRIAYLSGY) was synthesized, purified by high-pressure liquid chromatography, and verified by mass spectrophotometry by the Macromolecular Analysis Facility at the Albert Einstein College of Medicine. Peptides were coupled via their N-terminal cysteine residues to maleimide-activated keyhole limpet hemocyanin by using an Imject Activated Immunogen Conjugation Kit (Pierce). Male New Zealand White rab-

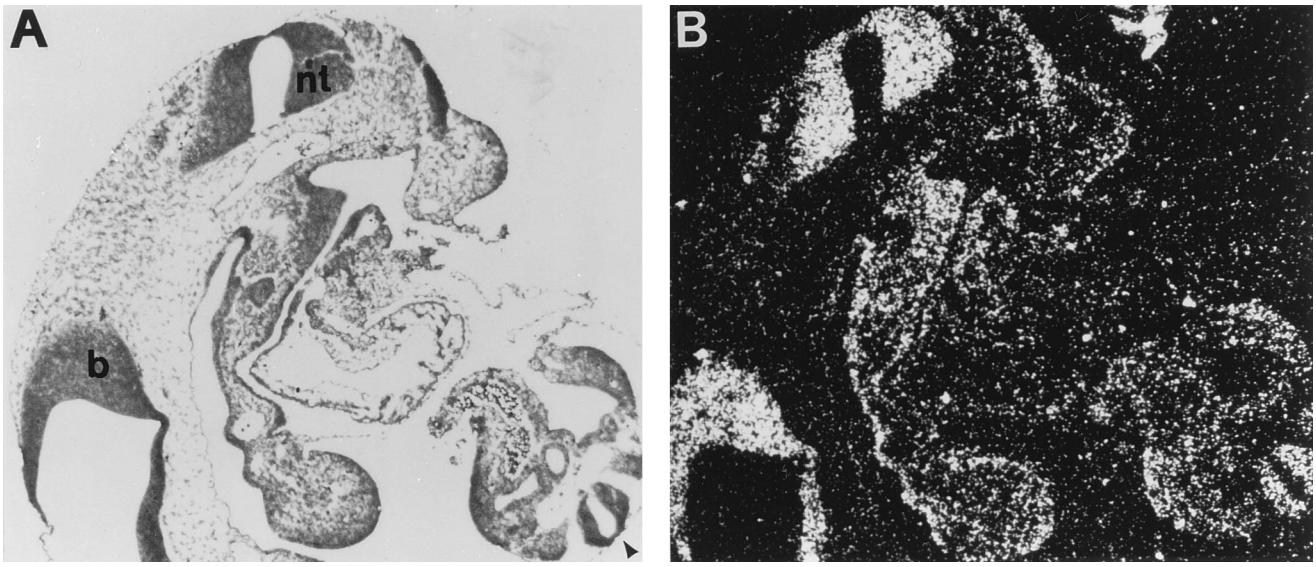

FIG. 1. L-*myc* expression at 9.5 days of embryogenesis. In situ hybridization of an L-*myc* antisense probe with a sagittal section of a 9.5-day-old mouse embryo revealed widespread expression in the neuroepithelium of the brain (b) and neural tube (nt and arrowhead). (A) Bright-field optics; (B) dark-field optics.

bits were immunized intradermally at multiple sites with the peptide-keyhole limpet hemocyanin conjugate in complete Fruend's (first booster) or reconstituted Ribi (Ribi Immunochem Research; subsequent boosters) adjuvant. The appearance of anti-L-Myc antibodies in the serum was monitored by dot blot analysis against peptide coupled to bovine serum albumin, and antibodies were affinity purified by chromatography on columns of L-Myc peptide linked to agarose beads (Ag/Ab Immunobilization Kit 2; Pierce).

For Western blotting analyses, fractions enriched with nuclei were prepared from newborn tissues by Dounce disruption in nuclear fractionation buffer (10 mM Tris-HCl [pH 7.5], 1 mM phenylmethylsulfonyl fluoride, 10 mM iodoacetamide, leupeptin [1 μg/ml], pepstatin A [1 μg/ml], aprotinin [2 μg/ml]). The pellets containing the nuclei were homogenized in 3% sodium dodecyl sulfate (SDS), and protein concentrations were analyzed by the method of Lowry et al. (37, 51). Protein samples were separated by SDS-polyacrylamide gel electrophoresis (PAGE) and transferred to nitrocellulose membranes. Membranes were blocked by incubation in PBS containing 10% nonfat dry milk and 0.1% Tween 20 (diluent) for 1 h at 37°C and then rinsed several times in PBS. Primary incubations of membranes were carried out with affinity-purified antibody at a 1:200 dilution in diluent, and secondary incubations were carried out with horseradish peroxidase-conjugated donkey anti-rabbit whole immunoglobulin G serum at a 1:5,000 dilution. Immunoreactive bands were visualized with an enhanced chemiluminescence kit (Amersham). Controls for nonspecific binding were prepared by preincubating the anti-L-Myc antiserum (at 1:50 dilutions) with its corresponding synthetic peptide linked to agarose beads (Ag/Ab Immunobilization Kit 2; Pierce) for 48 h at 4°C. After centrifugation, a 1:200 dilution of the supernatant was used as the primary antibody in place of the affinity-purified antibody.

Detection of cytoplasmic pigmented granules in neurons by EM. Animals were anesthesized and perfused with PBS followed by Trump's fixative. The cerebellum was dissected, postfixed for 30 min, dehydrated, and embedded in Epon. Preliminary sagittal sections were cut, mounted on microslides, and stained for light microscopy, and areas with appropriate structures were identified. The cervical spinal chord (about C1-2) was dissected and similarly processed. Spinal cords were cut into cross sections at angles perpendicular to the long axis. The Epon blocks were then trimmed with reference to the test sections, and EM sections were cut and mounted on Formvar-coated EM grids. Cerebellar Purkinje neurons were identified by the following criteria: their location in between the molecular and granular layers, their large size, the presence of apical dendrites, and the presence of the apical depression in the nuclear membrane (the nuclear depression is often filled with Golgi apparatus endoplasmic reticulum). Ventral motor neurons were identified by location and size. In both Purkinje neurons and ventral motor neurons, the number of cytoplasmic pigmented granules, identified by their darker staining compared with the staining of mitochondria, per neuron was counted. Only neurons visible as whole cells were analyzed. Neurons that were partially obscured (by the EM grid, for example) were not included in the analysis.

RESULTS

L-*myc* gene expression in the developing mouse embryo. The cellular expression of L-*myc* from early (E9.5) through midgestational (E15.5) stages of mouse development was determined by RNA in situ hybridization. At E9.5, the most prominent signals were detected throughout the neuroectoderm of the brain and neural tube (Fig. 1). By E12.5 and thereafter, abundant L-*myc* transcripts persisted throughout the central nervous system (CNS) and were also detected in the nasal epithelium, the metanephric kidney, and the developing lung buds (Fig. 2 and data not shown). These findings are in accord with those derived from previous Northern blot analyses, demonstrating that the newborn brain, kidney, and lung exhibit the highest levels of steady-state L-*myc* mRNA (74). Although the entire CNS was labeled in E12.5 (Fig. 2A to D) and E15.5 (Fig. 2E and F) embryos, some variation in labeling intensity was noted in certain areas with maturation of the CNS. For example, the ventral diencephalon (hypothalamus) (Fig. 2A and B) was labeled only slightly above the background, while other regions of the diencephalon, the telencephalon, and the neural tube were more strongly labeled (Fig. 2C and D). Similarly, the neuroepithelium of the medial cortex and septal areas of the telencephalon showed stronger signals than the more-lateral cortex and ganglionic eminence (Fig. 2E and F). Notably, L-*myc* expression was detected in the periventricular zone where cell proliferation takes place, as well as in more-lateral postmitotic regions (intermediate zone) where differentiation occurs. However, the most robust expression of L-*myc* was seen in the sensory nasal (olfactory) epithelium (Fig. 2G and H). Expression was also detected in the epithelium of the esophagus, trachea, thymic rudiment, and liver at 15.5 days (data not shown). Consistent with previous studies, strong L-*myc* expression in the developing metanephric kidney at midgestation localized to the large papillary ducts of the collecting duct system, papilla, renal pelvis, and ureter (data not shown) (48). These previous studies also demonstrated that L-*myc* expression persists in the adult ureter, wherein the continual renewal of epithelium takes place (48). The localization of L-*myc* ex-

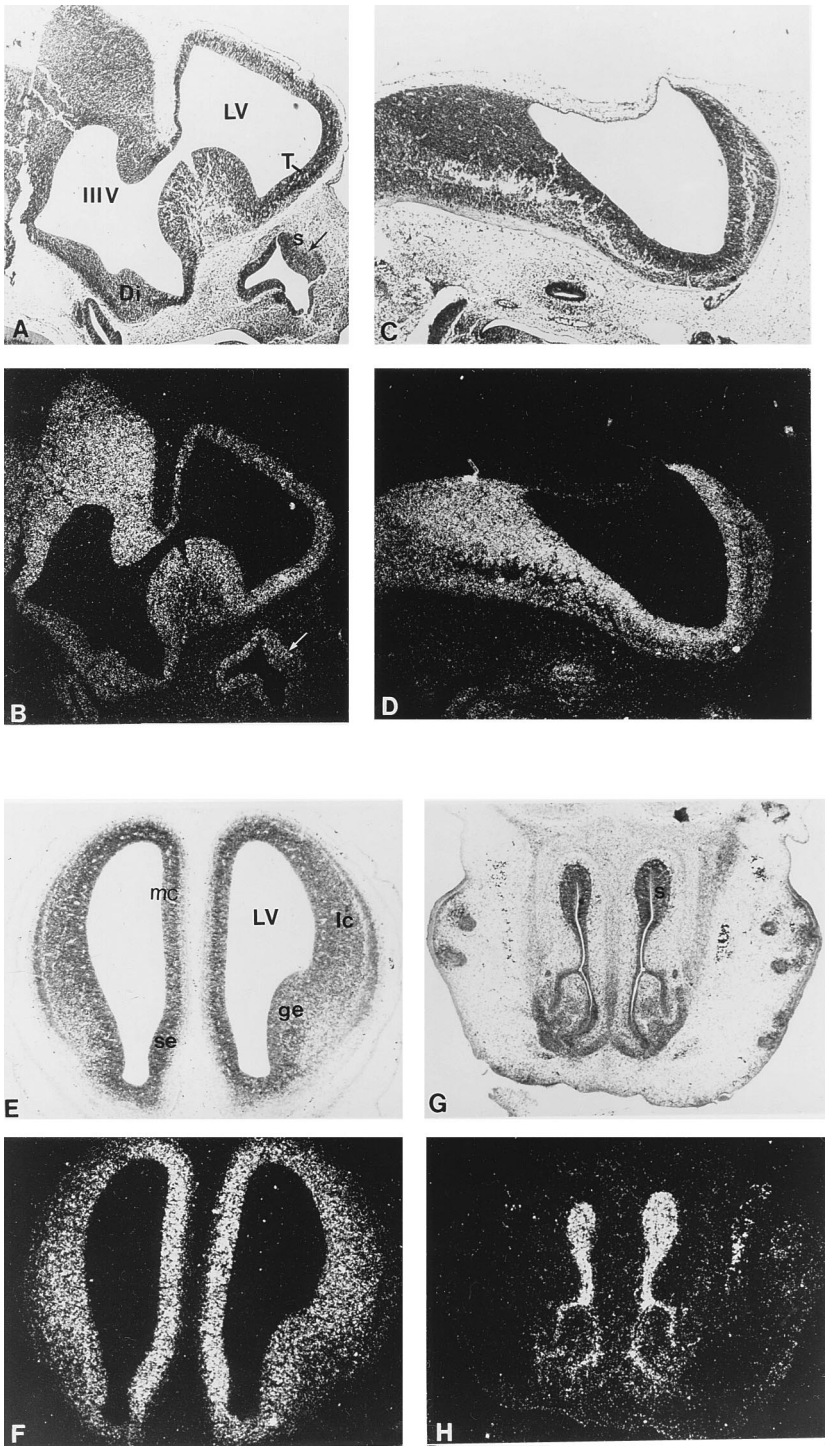

FIG. 2. L-*myc* expression in midgestational embryos. L-*myc* in situ hybridization with sections of 12.5 (A to D)- and 15.5 (E to H)-day-old mouse embryos showed expression in the developing CNS and sensory nasal epithelium. (A and B) A sagittal section of a 12.5-day-old embryo showed expression in the forebrain. Note that the signal intensity over the ventral diencephalon is much lower than it is in other regions. The neurogenic sensory nasal epithelium, but not the nonneurogenic respiratory nasal epithelium, showed label. The arrow demarcates the boundary between the sensory epithelium and the respiratory epithelium. (C and D) Expression was seen in the neuroectoderm of the hindbrain and neural tube in a sagittal section of a 12.5-day-old mouse embryo. (E and F) Frontal section through a 15.5-day-old embryo showing differential expression in the neuroectoderm of the telencephalon, with the highest concentration of grains over the septal and medial cortex areas. (G and H) Frontal section through the snout showing robust labeling of the sensory nasal epithelium. (A, C, E, and G) Bright-field optics. (B, D, F, and H) Dark-field optics. T, telencephalon; Di, diencephalon; LV, lateral ventricle; IIIV, third ventricle; s, sensory olfactory epithelium; ge, ganglionic eminence; lc, lateral cortex; mc, medial cortex; se, septal area.

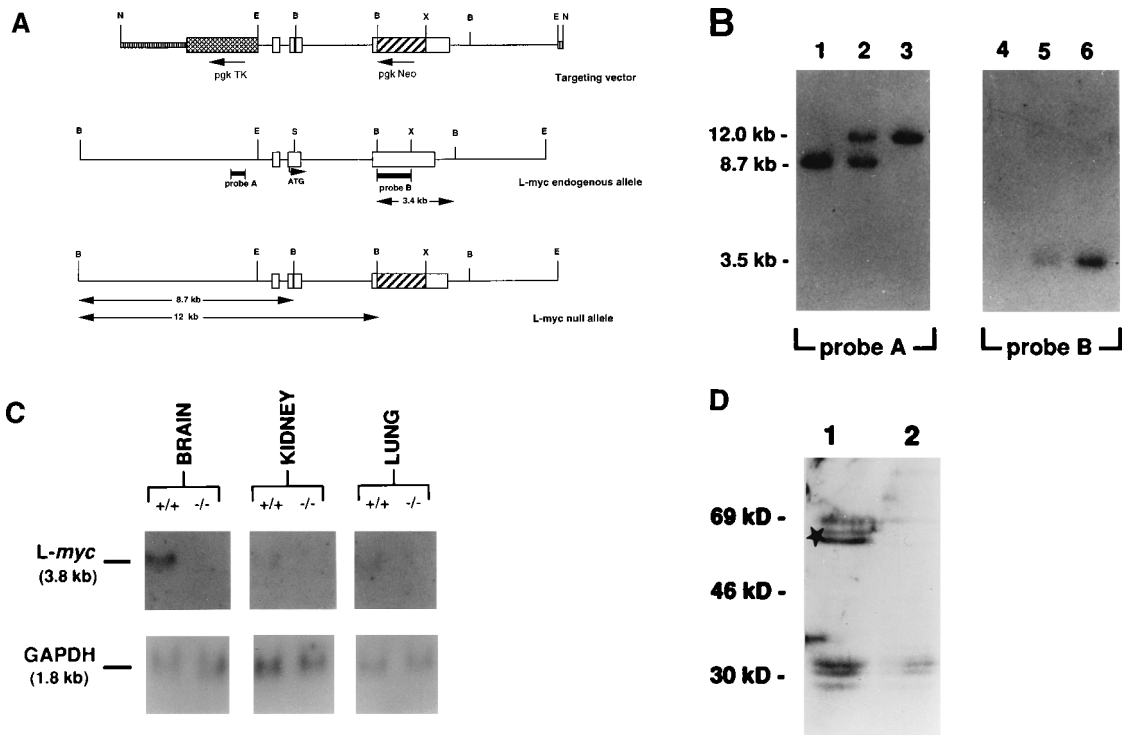

FIG. 3. (A) The L-*myc* gene is organized into three exons. Exon 1 encodes the 5′ untranslated region and a portion of a non-AUG-initiated open reading frame; exon 2 contains an in-frame AUG-initiated open reading frame which encodes the putative transactivation domain; and the remainder of the ORF which encodes the nuclear localization signals and the bHLH/LZ structure is found on exon 3 and is followed by a long 3′ untranslated region. Two 19-bp oligonucleotides (CGTGAATAG GATCCGATAG and CGCTATCGGATCCTATTCA) were annealed and ligated into the *Bst*BI site at position 1531 in the L-*myc* second exon. This oligonucleotide introduces a new *Bam*HI restriction site and causes a frameshift mutation which results in premature termination of translation in the second exon. The Neo^r gene was corrected to wild-type sequences by cloning a *Nar*I-*Nco*I fragment containing wild-type sequences into the mutated Neo^r gene. The Neo^r and herpes simplex virus thymidine kinase (TK) genes were placed in the opposite transcriptional orientation relative to that of the L-*myc* gene. N, *Nde*I; E, *Eco*RI; B, *Bam*HI; X, *Xho*I; S, *Bst*BI. (B) Southern blot depicting genotypes obtained from heterozygous null L-*myc* intercrosses. Tail DNA of offsprings from heterozygous null intercrosses was digested with *Bam*HI, fractionated through 0.8% agarose, and transferred to nitrocellulose membranes. Probe A was an 800-bp *Eco*RI segment located 5′ to L-*myc* sequences, and probe B was the *Bam*HI-to-*Xho*I deleted fragment depicted in panel A. Lanes 1 and 4, DNA from homozygous null L-*myc* mice; lanes 2 and 5, DNA from heterozygous null L-*myc* mice; lanes 3 and 6, DNA from wild-type mice. (C) Northern blot analysis of L-*myc* expression in tissues from normal (+/+) and homozygous null (−/−) L-*myc* mice. The probe for L-*myc* was probe B, the *Bam*HI-to-*Xho*I deleted fragment depicted in Fig. 3A. (D) Western blot analysis of L-Myc expression in homogenates of newborn brain tissue from wild-type (lane 1) and homozygous null mutant (lane 2) mice. The star indicates the L-Myc-specific doublet. Portions (50 μg) of protein lysates from nuclear fractions were fractionated on SDS–7.5% PAGE gels, transferred to nitrocellulose, and incubated with affinity-purified anti-L-Myc antisera.

pression to these organs suggests a role therein. To examine this possibility more directly, we assessed the developmental consequences of L-*myc* gene inactivation in the mouse.

Targeted disruption of the L-*myc* gene in ES cells and transmission through the germ line. A 12.0-kb *Eco*RI L-*myc* fragment derived from a BALB/c genomic library (36) served as a source of L-*myc* homologous sequences for the production of a positive/negative replacement-type vector (41) (Fig. 3A). Two modifications served to disrupt the L-*myc* open reading frame. First, a 19-bp oligonucleotide introduced a *Bam*HI site and a translational terminator into the second-exon region encoding the amino-terminal transactivation domain. Second, a third-exon 1.4-kb *Bam*HI-*Xho*I fragment encoding nuclear localization, bHLH/LZ, and some 3′ untranslated sequences was replaced completely by the neomycin resistance (Neo^r) gene under the control of the phosphoglycerokinase 1a (*pgk*) promoter and polyadenylation signal. A *pgk*-driven herpes simplex virus thymidine kinase gene was placed in a flanking position to permit selection, in the presence of ganciclovir, against random integration events.

All of the mutant ES cells used to generate null L-*myc* mice were derived from two electroporations of 5×10^7 cells each as detailed in Materials and Methods. In the two electroporations, selection generated approximately 5,600 and 3,600 Neomycin-resistant colonies versus 925 and 1570 doubly resistant colonies, respectively, yielding enrichments of 6.1- and 2.3-fold by counterselection. A total of 217 doubly resistant clones were subjected to Southern blot analysis. In a homologous recombination event, L-*myc*-Neo^r gene integration results in (i) the introduction of a *Bam*HI site in the second exon that decreases a *Bam*HI genomic band from 12 kb to 8.7 kb and (ii) the deletion of the bHLH/LZ region of the third-exon sequences detected by probe B (Fig. 3A), producing a null allele. Four mutant clones that contained restriction fragment length alterations consistent with a targeted event were identified (see below). Injections into C57BL/6 blastocysts generated chimeric mice with agouti coat color contributions ranging from 30 to 100%. Upon mating with C57BL/6 partners, chimeric mice generated with three of these clones produced agouti offspring harboring the mutant L-*myc* allele.

L-Myc-deficient mice are viable and apparently healthy. To ascertain whether L-Myc plays an essential role in development, genotype distribution was determined for offspring generated from heterozygous null L-*myc* intercrosses. All three genotypes were represented (Fig. 3B, probe A), and they were distributed at a ratio of 1:2:1 for both 100 embryos spanning

E9.5 through E18.5 and over 300 live offspring. There were no consistent congenital defects that correlated with a specific genotype in the embryonic and adult samples, as assessed by visual inspection and more detailed studies (see below). In addition to a normal genotype distribution, the likelihood that perinatal lethality was associated with L-Myc deficiency was ruled out by careful monitoring of the births of many litters. The homozygous null L-*myc* mice have a life span comparable to that of their heterozygous and wild-type littermates, surviving over 2 years without evidence of specific physiological compromise. Furthermore, examination of the genotypes resulting from spontaneous deaths in the total mouse population over a 3-year period revealed that the homozygous null L-*myc* mice were not overrepresented or underrepresented in this subpopulation. Homozygous null L-*myc* mice produced phenotypically normal offspring.

Given the lack of a gross impact on viability, disruption of the L-*myc* gene was verified on three levels. By Southern analysis, L-*myc* exon 3 sequences that were replaced by the Neo^r gene were completely absent from the homozygous null mouse genome, as determined by hybridization with probe B (Fig. 3B, probe B, lane 4). Similarly, Northern blot studies of a panel of newborn tissues derived from homozygous null L-*myc* mice failed to detect L-*myc* transcripts when the probe directed to the deleted L-myc sequences (probe B) was used (Fig. 3C). Lastly, Western blotting demonstrated that the 62-kDa–68-kDa L-Myc protein doublet was absent in homozygous null L-*myc* brain lysates (Fig. 3D; compare starred bands in lane 1 with lane 2).

Normal growth and morphological development in L-Myc-deficient mice. An extensive histological survey was performed on adult tissues from wild-type and homozygous null L-*myc* mice with a particular emphasis on tissues that express L-*myc* during development—those of the forebrain, cerebellum, lung, kidney, and gastrointestinal tract. A comparative histological analysis of one pair of wild-type and null L-*myc* mice at E15.5, E18.5, and adult stages did not reveal any obvious differences in morphology or cellularity (Fig. 4; only the adult stage is shown). In particular, cytoarchitecture and cell numbers were similar in the CNS (Fig. 4A and B). In contrast to that of the lungs of mice homozygous for a hypomorphic allele of the N-*myc* gene (42) or a null N-*myc* mutation (58, 66), the bronchiolar branching pattern of the lungs of L-Myc-deficient mice was normal and type I and type II pneumocytes were well represented (Fig. 4C). The kidney had normal numbers of glomeruli and cortical thickness, and the collecting ducts appeared normal (Fig. 4D). The morphology of the villi in the small intestine, as well as the liver, also appeared unaffected (Fig. 4E and F, respectively).

The observations that L-*myc* expression is deregulated in some naturally occurring tumors and that L-*myc* exhibits oncogenic activity in the rat embryo fibroblast assay prompted a detailed examination of cellular proliferation in embryonic tissues that normally express detectable levels of L-*myc* mRNA during development. A BrdU immunoperoxidase histochemical assay was used to visualize cells progressing through S phase in organs of 15.5-day-old embryos following a 1-h pulse with BrdU in utero. Comparison of wild-type and homozygous null L-*myc* littermates showed no obvious differences in numbers and distribution of S-phase nuclei in L-*myc*-expressing tissues such as those of the kidney, the periventricular zone in the cerebellar cortex, or the olfactory epithelium (Fig. 5). Significantly, the strong labeling of the nasal epithelium in the in situ studies prompted a closer examination of the nasal epithelium. The nasal epithelium appeared normal upon gross examination in the homozygous null mice; however, this observation does not rule out some subtle changes in the olfactory epithelium that could escape detection by these methods. Additionally, these results support our previously stated hypothesis that L-Myc does not play a prominent role in the regulation of cellular proliferation during normal development (44).

Studies with cell culture and during normal development have shown that dramatic changes in *myc* family gene expression often accompany key differentiation events, and aberrant expression of each *myc* family gene has been shown to impair differentiation in cell culture systems of differentiation and in transgenic mice (for a review, see reference 43). In particular, overexpression of L-*myc* in cultured neuroblasts has suggested a specific role for L-Myc in early CNS development as a factor that guides immature multipotent neuroblasts towards a neuronal rather than a glial cell type (7). Although the histological survey of the adult CNS failed to uncover any defects in neuronal development, the developmental plasticity of the CNS could obscure early developmental perturbations. To this end, CNS development was assayed on the molecular level through an examination of neurofilament protein NF-66 expression during embryonic neuronal development. NF-66 was selected as a neuronal marker since it is abundantly expressed in neurons of embryonic and postnatal brain tissue and is highly specific and well characterized (15, 23). Immunocytochemical studies of NF-66 clearly showed that its expression and distribution in neuronal cytoarchitecture were virtually indistinguishable between wild-type and homozygous null L-*myc* mice (Fig. 6). These findings, coupled with the normal histological appearance of the CNS, argue against an essential and unique role for L-Myc in early neuronal development.

The high level of L-*myc* gene expression in the developing mouse CNS (74) and the chromosomal localization of the human L-*myc* gene to the vicinity of the candidate locus for the infantile form of Batten's disease (CNL1) (26) prompted a careful ultrastructural examination of the brains of L-Myc-deficient mice for pathognomonic features of this disease. In humans, Batten's disease is characterized by progressive mental retardation, seizures, retinal degeneration, and cortical atrophy. On the cellular level, a hallmark pathological feature is the accumulation of clustered ceroid lipofuscin inclusions (reviewed in references 27 and 54), clearly evident in large neurons such as those of the cerebellum and the ventral motor horn of the spinal cord. Ultrastructural analysis of the cerebella and cervical spinal cords of age-matched wild-type and homozygous null L-*myc* adults did not detect any significant increase in the number or size of lipofuscin inclusions (data not shown). These findings are consistent with a recent report citing mutations in the closely linked palmitoyl protein thioesterase gene as the causative genetic alteration in the infantile form of Batten's disease (70).

Expression of c-*myc* and N-*myc* genes in homozygous null L-*myc* tissues. The lack of a gross phenotype associated with L-Myc deficiency could be the result of compensation by other members of the Myc family. Indeed, disruption of the N-*myc* gene has been shown to be associated with a rise in the level of expression of c-*myc* in the neuroepithelium of the developing CNS (66). In order to determine whether alterations in *myc* family gene expression occurred in homozygous null L-*myc* tissues, Northern blot and RNA in situ hybridization studies assayed the levels and patterns of c- and N-*myc* in tissues that normally express abundant levels of L-*myc*. Northern blot analyses of total RNA derived from the newborn brain, kidney, lung, and skin demonstrated that similar ranges of steady-state c- and N-*myc* expression were present in wild-type and null L-*myc* samples (Fig. 7; only data for c-*myc* are shown). Simi-

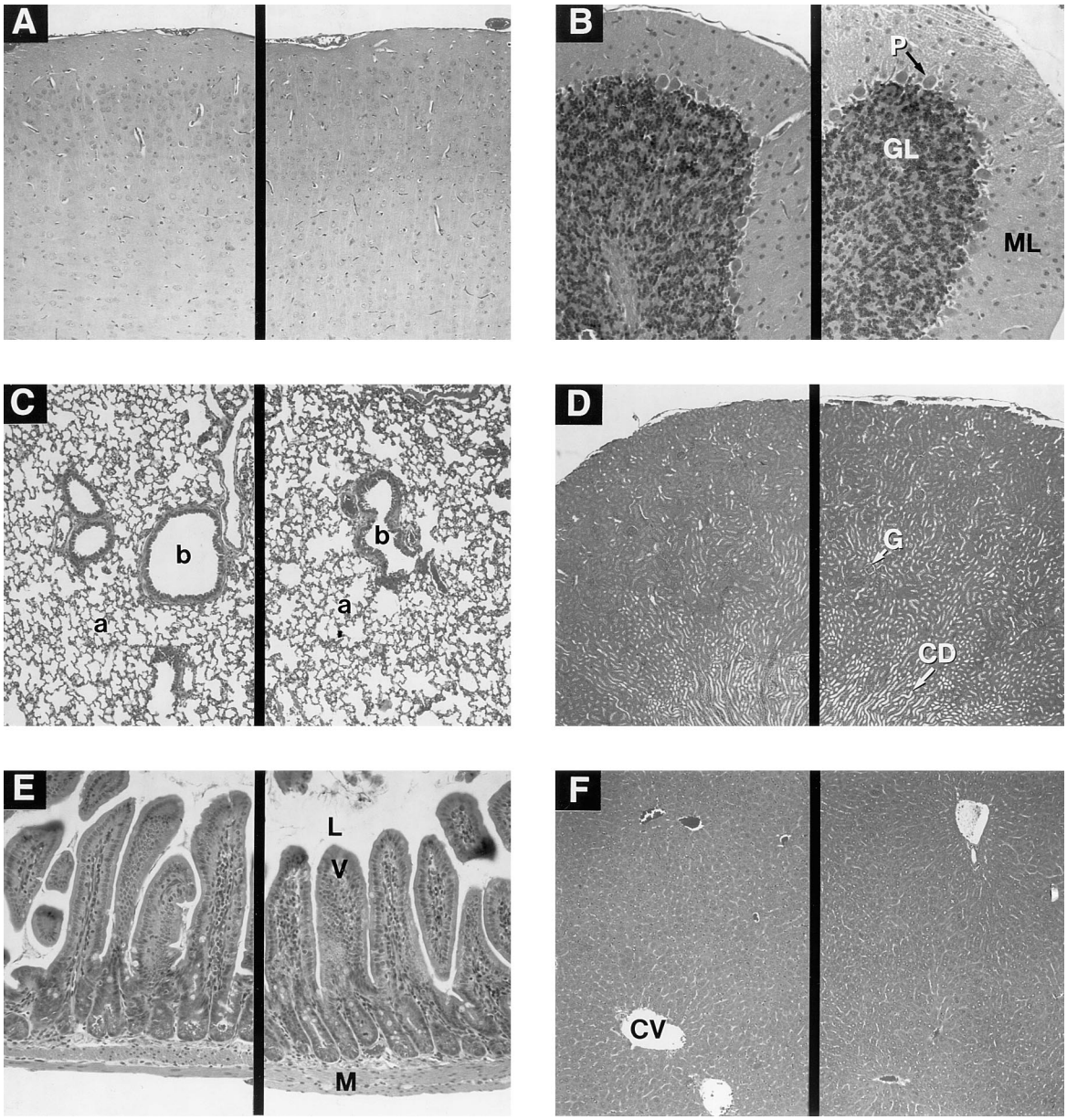

FIG. 4. Histological survey of tissues from wild-type (left panels) and homozygous null mutant (right panels) mice. Hematoxylin-and-eosin-stained sections of cortex (A), cerebellum (B), lung (C), kidney (D), intestine (E), and liver (F) from 2-month-old littermates are shown. P, Purkinje cell; GL, granular layer; ML, molecular layer; a, alveoli; b, bronchus; G, glomerulus; CD, collecting ducts; L, intestinal lumen; V, villus; M, muscular layer; CV, central vein.

larly, RNA in situ hybridization analysis of E15.5 embryo sections demonstrated that both the levels and the cellular distributions of c-*myc* and N-*myc* transcripts were approximately the same in wild-type, homozygous, and heterozygous null L-*myc* samples (data not shown).

DISCUSSION

Previous biochemical and biological studies have implicated L-Myc as an important regulator involved in governing the growth and development of diverse cell types. From the standpoint of oncogenesis, overexpression of L-*myc* has been associated with malignant transformation in naturally occurring tumors, in cultured cells, and in transgenic mice (reviewed in reference 43). Enforced high-level expression of L-*myc* perturbs differentiation in the lens (44), the thymus (45, 46), and cultured erythroleukemia cells (8), suggesting that a regulated pattern of developmental stage-specific expression of L-*myc* is a requirement for normal cellular differentiation. The detrimental effects of forced L-*myc* overexpression seem to underscore the importance of normal physiological levels of L-*myc* in developing tissues. A well-defined primary cell culture system to potentially study the effects of a loss-of-function L-*myc* mutation on differentiation or cell cycle effects has not yet been developed because of the low level of L-*myc* expression in normal cells. Therefore, we have focused on the in vivo effects of absent L-Myc function. The elimination of L-Myc function might therefore be expected to cause significant perturbations in tissues that normally express detectable levels of L-*myc* (such as cerebellar cortex, cerebellum, lung, kidney, and intes-

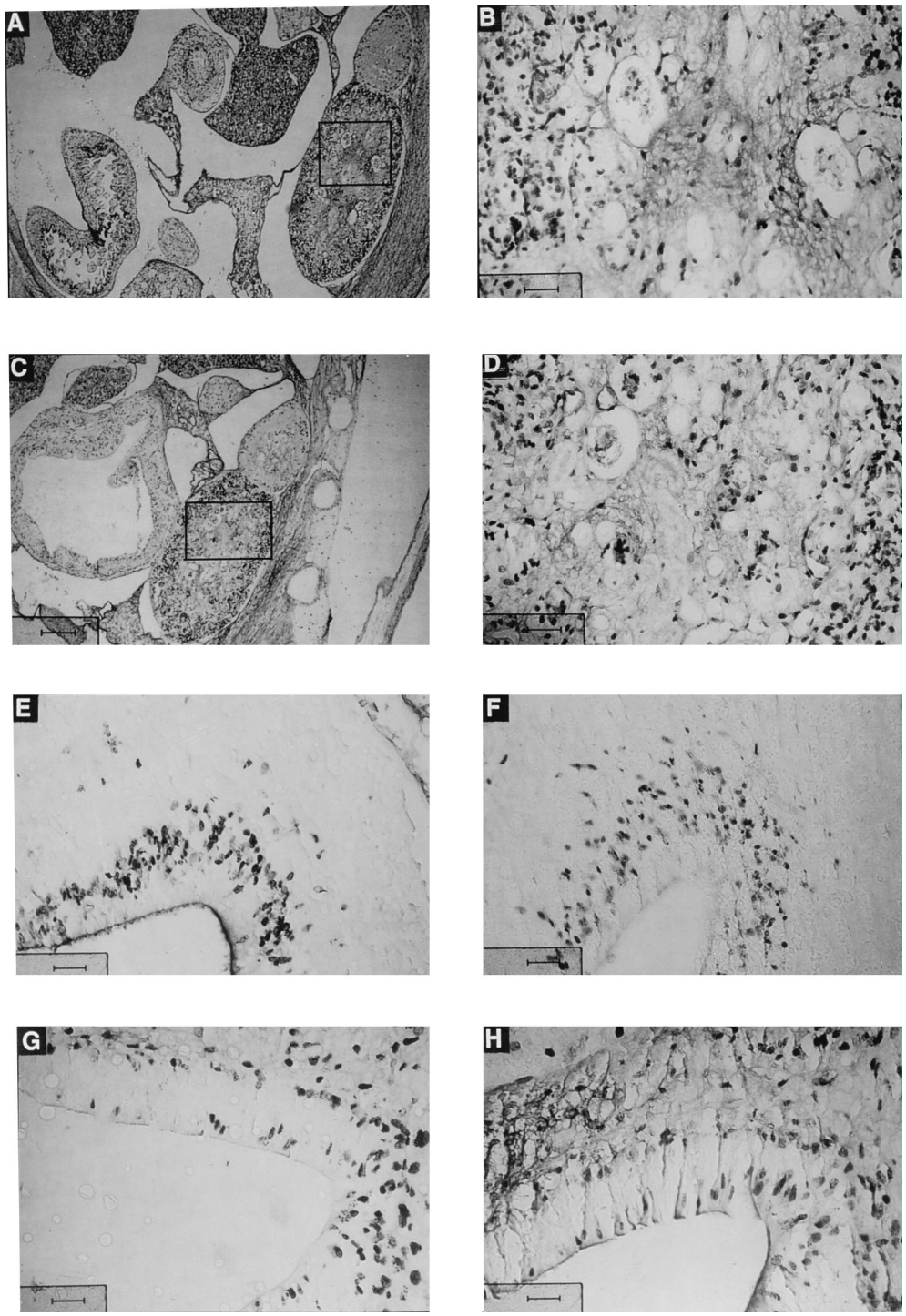

FIG. 5. Sections through 15.5-day-old tissues from BrdU-treated wild-type (A, B, E, and G) and homozygous null (C, D, F, and H) L-*myc* embryos were assayed by indirect immunoperoxidase methods using an anti-BrdU antibody. (A and C) Wild-type and homozygous null L-*myc* whole embryos, respectively; (B and D) higher-magnification images of embryonic kidneys of wild-type and homozygous null L-*myc* mice, respectively, as demarcated by the boxes in panels A and C; (E and F) the forebrain periventricular region; (G and H) the olfactory epithelium.

tine tissues). However, the studies described here, in which the L-*myc* gene was specifically disrupted by homologous recombination, demonstrate that L-*myc* joins an expanding list of genes whose inactivation fails to generate significant pathophysiological consequences (13, 56, 57).

Homozygous null L-*myc* mice are viable and fertile and thrive well into adulthood. On the gross morphological level, tissues that normally express the L-*myc* gene were not affected by the loss of L-Myc. These results contrast with those observed previously for c-*myc* and N-*myc* mutations, wherein a homozygous null background was associated with embryonic lethality (14, 16, 58, 66). Correspondingly, the normal neuronal

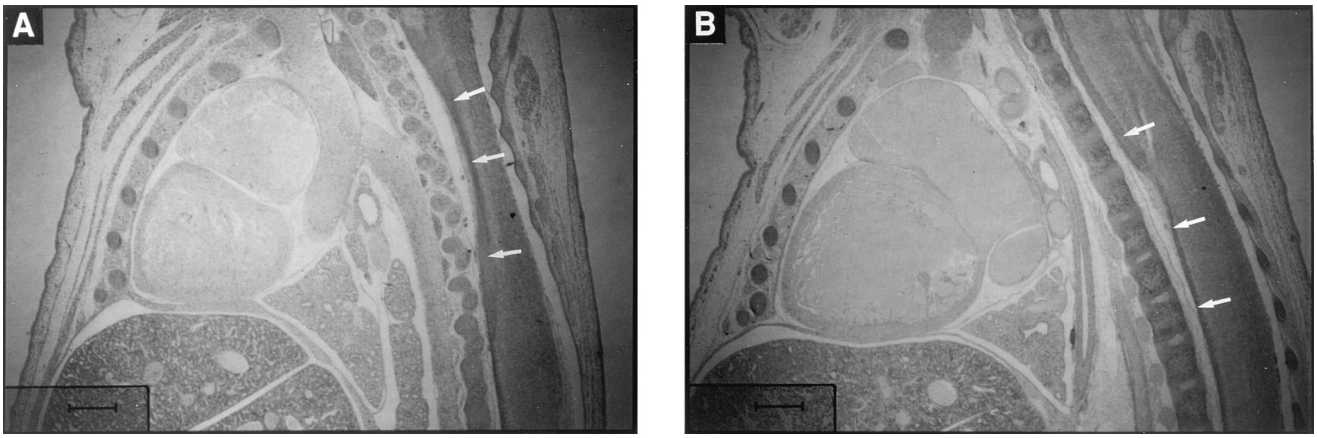

FIG. 6. Immunohistochemical detection of NF-66 in E18.5 wild-type (A) and homozygous null mutant (B) embryos. The arrows indicate regions of NF-66 staining along cortical spinal tracts.

cytoarchitecture and developmentally regulated pattern of the NF-66 neurofilament marker in L-Myc-deficient mice further negates the view that L-Myc plays a unique and essential role in the development of neurons. These results contrast sharply with those obtained in recent cell culture studies in which overexpression of L-*myc* stimulated bipotent neuroblasts to differentiate into a neuronal rather than a glial cell type (7). A possible basis for this L-*myc*-induced neuronal differentiation may relate to the ability of weakly transactivating L-Myc to antagonize the growth-promoting activities of c-Myc, perhaps through the competitive occupation of consensus sites in common Myc-responsive gene targets. Specifically, L-*myc* has been shown to diminish the transforming potential of c-Myc to a level intermediate between those of c-Myc and L-Myc by themselves (49). Since c-Myc function appears to be required for cellular proliferation, the overexpression of L-Myc could cause cycling, immature neuroblasts to withdraw from the cell cycle, thus precipitating neuronal differentiation by default. Indeed, many agents or conditions which bring about mitotic arrest of immature neuroblasts frequently result in their terminal differentiation into neurons.

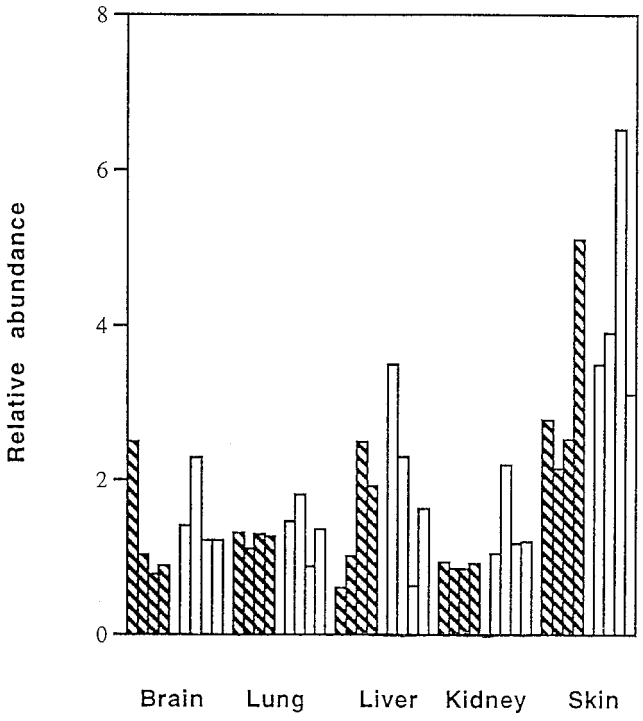

FIG. 7. Histogram depicting the levels of c-*myc* in tissues from individuals after correction for RNA loading with GAPDH. The histogram was derived from autoradiograms of Northern blot analysis of *myc* gene expression in newborn brain, lung, liver, kidney, and skin tissues from wild-type and homozygous null L-*myc* mice. The same membrane was hybridized with c-*myc*, dehybridized, and reprobed with GAPDH. A separate filter was hybridized, dehybridized, and probed with N-*myc*, L-*myc*, and GAPDH (data not shown). ▨, +/+; □, −/−.

The apparent dispensability of L-Myc suggests that if L-Myc does indeed play a functional role in embryonic or postnatal development, c-Myc, N-Myc, the increase in the intracellular concentration of Max, or a compensatory increase in the Max-associated proteins Mad and Mxi may likely compensate for this role when L-Myc is absent. Possible complementation among members of the Myc family appears plausible and derives support from a number of observations. On the biochemical level, all three Myc oncoproteins dimerize with Max (1, 11, 12, 23, 49, 71) and bind the same consensus recognition sequence, CACGTG (10, 25, 31, 39, 53). In more-biological assays, transactivation-incompetent mutants of one Myc member act in *trans* to dominantly suppress the cotransformation activities of all three Myc oncoproteins, indicating that the Myc family members function through common genetic elements to transform normal cells (49). Moreover, with respect to *myc* family gene expression in development, c- and N-*myc* exhibit distinct cell-type-specific differences in many organs (21, 47, 66, 74), while L-*myc* is typically coexpressed with at least one other *myc* family gene (48, 74). Consequently, the differential expression of c- and N-*myc* in developing organ systems may provide a basis for the midgestational lethality associated with homozygous null c-*myc* or N-*myc* genotypes, while the coordinate expression in the case of L-*myc* may facilitate its rescue by other members in L-Myc-deficient mice through elimination of the requirement for alterations in the cell-type-specific expression of c- or N-*myc*. Finally, the negligible effect of the loss of L-Myc may relate to its relatively weak transactivation potential (17) and its possible role as a subtle regulator of Myc-responsive growth and differentiation genes. In this regard, the principal role of L-Myc may be to function as an attenuator, rather than an activator, of these Myc-responsive gene targets, serving to modulate the regulatory activities of the more potent c- and N-Myc proteins. In this case, the loss of a negative

regulator may have few consequences for development and may be manifested only as an enhanced predisposition to Myc-induced malignant disease, a possibility that remains to be determined. Such a precedent has been established for an important negative regulator of cell cycle progression, the p53 tumor suppressor gene product (20). If this alternative explanation is correct, compensatory mechanisms for the loss of L-Myc may have little or no impact on the expression of c- and N-*myc* in tissues which normally express L-*myc*; this prediction is substantiated by results obtained in expression studies of the developing and newborn tissues of the homozygous null L-*myc* mouse (see above).

Complementary and distinct activities of members of the Myc family will be further clarified by the production and phenotypic analysis of homozygous null c- and/or N-*myc* genotypes against an L-Myc-deficient background. The outcome of such experiments will be particularly useful for discerning the potential role of the Myc family in early embryonic growth and development. These studies, coupled with the analysis of mice deficient in Max or Max-associated proteins (Mad and Mxi1), will also help to elucidate how this network of molecules interacts and functions to bring about orchestrated patterns of developmental gene expression during mammalian embryogenesis.

ACKNOWLEDGMENTS

J.H. was supported by a Cancer Center Core NIH grant (2P30CA 13330). S.D.M. and H.-W.L. are supported by an NIH training grant (CA09173). D.P. and F.-C.C. are supported by grants NS23840 and NS23705. K.S.H. was supported initially by a postdoctoral fellowship from an NIH Immunoncology Training grant (CA09173) and more recently by an NSF grant (IBN-9304602) and the Markey Charitable Trust. Partial support for mouse housing was obtained through the core program on carcinogenesis (5-P30-CA12227) at Temple University School of Medicine. R.A.D. is a recipient of an American Heart Association Investigator Award and the Irma T. Hirschl Award and is supported by NIH grants EY09300 and HD28317 and by a research grant from the March of Dimes.

We thank Salome G. Waelsch, Keith Latham, Nicole Schreiber-Agus, and Raju Kucherlapati for critically reading the manuscript; Asao Hirano for his insight and advice on the ultrastructural analysis; and Leena Peltonen for alerting us to a possible connection between L-*myc* and Batten's disease. Yvonne Kress is acknowledged for assistance in electron microscopy, and the excellent technical assistance of Musen Liang is gratefully acknowledged.

REFERENCES

1. **Amati, B., M. W. Brooks, M. Levy, T. D. Littlewood, G. I. Evan, and H. Land.** 1993. Oncogenic activity of the c-*myc* protein requires dimerization with Max. Cell **72:**233–245.
2. **Amati, B., S. Dalton, M. W. Brooks, T. D. Littlewood, G. I. Evan, and H. Land.** 1992. Transcriptional activation by the human c-Myc oncoprotein in yeast requires interaction with Max. Nature (London) **359:**423–426.
3. **Auffray, C., and F. Rougeon.** 1980. Purification of mouse immunoglobulin heavy chain messenger RNAs from total myeloma tumor RNA. Eur. J. Biochem. **107:**303–314.
4. **Barrett, J., M. J. Birrer, G. J. Kato, H. Dosaka-Akita, and C. V. Dang.** 1992. Activation domains of L-Myc and c-Myc determine their transforming potencies in rat embryo cells. Mol. Cell. Biol. **12:**3130–3137.
5. **Benvenisty, N., A. Leder, A. Kuo, and P. Leder.** 1992. An embryonically expressed gene is a target for c-*myc* regulation via the c-*myc* binding sequence. Genes Dev. **6:**2513–2523.
6. **Berberich, S. J., and M. Cole.** 1991. Casein kinase II inhibits the DNA binding activity of Max homodimers but not Myc/Max heterodimers. Genes Dev. **6:**166–176.
7. **Bernard, O., J. Drago, and H. Sheng.** 1992. L-*myc* and N-*myc* influence lineage determination in the central nervous system. Neuron **9:**1217–1224.
8. **Birrer, M. J., L. Raveh, H. Dosaka, and S. Segal.** 1989. A transfected L-*myc* gene can substitute for c-*myc* in blocking murine erythroleukemia differentiation. Mol. Cell. Biol. **9:**2734–2737.
9. **Birrer, M. J., S. Segal, J. S. DeGreve, F. Kaye, E. A. Sausville, and J. D. Minna.** 1988. L-*myc* cooperates with *ras* to transform primary rat embryo fibroblasts. Mol. Cell. Biol. **8:**2668–2673.
10. **Blackwell, K., L. Kretzner, E. M. Blackwood, R. N. Eisenman, and H. Weintraub.** 1990. Sequence-specific DNA binding by the c-*myc* protein. Science **250:**1149–1151.
11. **Blackwood, E., and R. N. Eisenman.** 1991. Max: a helix-loop-helix zipper protein that forms a sequence-specific DNA binding complex with Myc. Science **251:**1211–1217.
12. **Blackwood, E. M., B. Luscher, and R. N. Eisenman.** 1992. Myc and Max associate *in vivo*. Genes Dev. **6:**71–80.
13. **Bueler, H., M. Fischer, Y. Lang, H. Bluethmann, H.-P. Lipp, S. J. DeArmond, S. B. Prusiner, M. Aguet, and C. Weissmann.** 1992. Normal development and behavior of mice lacking the neuronal cell-surface PrP protein. Nature (London) **356:**577–581.
14. **Charron, J., B. Malynn, P. Fisher, V. Stewart, L. Jeannotte, S. P. Goff, L. Robertson, and F. W. Alt.** 1992. Embryonic lethality in mice homozygous for a targeted disruption of the N-*myc* gene. Genes Dev. **6:**2248–2257.
15. **Chiu, F.-C., E. A. Barnes, K. Das, J. Haley, P. Sokolow, P. Macaluso, and J. Fant.** 1989. Characterization of a 66 kD subunit of mammalian neurofilaments. Neuron **2:**1435–1445.
16. **Davis, A. C., M. Wims, G. D. Spotts, S. Hann, and A. Bradley.** 1993. A null c-*myc* mutation causes lethality before 10.5 days of gestation in homozygotes and reduced fertility in heterozygous female mice. Genes Dev. **7:**671–682.
17. **DePinho, R. A., K. S. Hatton, A. Tesfaye, G. D. Yancopoulos, and F. W. Alt.** 1987. The human *myc* gene family: structure and activity of L-*myc* and an L-*myc* pseudogene. Genes Dev. **1:**1311–1326.
18. **DePinho, R. A., E. Leguoy, L. B. Feldman, N. E. Kohl, G. D. Yancopoulos, and F. W. Alt.** 1986. Structure and expression of the murine N-*myc* gene. Proc. Natl. Acad. Sci. USA **83:**1827–1831.
19. **DePinho, R. A., N. Schreiber-Agus, and F. W. Alt.** 1991. *Myc* family oncogenes in the development of normal and neoplastic cells. Adv. Cancer Res. **12:**1–46.
20. **Donehower, L. A., M. Harvey, B. L. Slagle, M. J. McArthur, C. J. Montgomery, J. S. Butel, and A. Bradley.** 1992. Mice deficient for p53 are developmentally normal but susceptible to spontaneous tumors. Cell **70:**937–948.
21. **Downs, K. M., G. R. Martin, and J. M. Bishop.** 1989. Contrasting patterns of *myc* and N-*myc* expression during gastrulation of the mouse embryo. Genes Dev. **3:**860–869.
22. **Evan, G. I., and T. D. Littlewood.** 1993. The role of c-*myc* in cell growth. Curr. Biol. **3:**44–49.
23. **Galinovic-Schwartz, V., D. Peng, F.-C. Chiu, and T. R. Van De Water.** 1991. Temporal pattern of innervation in the developing mouse ear and immunocytochemical study of a 66 kD subunit of mammalian neurofilaments. J. Neurosci. Res. **30:**124–133.
24. **Handyside, A. H., G. T. O'Neill, and M. L. Hooper.** 1989. Use of BRL-conditioned medium in combination with feeder layers to isolate a diploid embryonal stem cell line. Roux's Arch. Dev. Biol. **198:**48–55.

24a. **Hatton, K. S., and R. A. DePinho.** Unpublished observations.

25. **Hazalonetis, T. D., and A. Kandil.** 1991. Determination of the c-Myc binding site. Proc. Natl. Acad. Sci. USA **88:**6162–6166.
26. **Hellsten, E., E. Vesa, M. C. Speer, T. P. Makels, I. Jarvela, K. Alitalo, J. Ott, and L. Peltonen.** 1993. Refined assignment of the infantile neuronal ceroid lipofuscinosis (INCL, CLN1) locus at 1p32: incorporation of linkage disequilibrium in multipoint analysis. Genomics **16:**720–725.
27. **Jolly, R. D., R. D. Martinus, and D. N. Palmer.** 1992. Sheep and other animals with ceroid-lipofuscinoses: their relevance to Batten's disease. Am. J. Med. Genet. **42:**609–614.
28. **Kato, G. J., J. Barret, M. Villa-Garcia, and C. V. Dang.** 1990. An amino-terminal c-Myc domain required for neoplastic transformation activates transcription. Mol. Cell. Biol. **10:**5914–5920.
29. **Kato, G. J., W. F. Lee, L. Chen, and C. V. Dang.** 1992. Max: functional domains and interaction with c-Myc. Genes Dev. **6:**81–92.
30. **Kaye, F., J. Battey, M. Nau, B. Brooks, E. Seifter, J. DeGreve, M. Birrer, E. Sausville, and J. Minna.** 1988. Structure and expression of the human L-*myc* gene reveal a complex pattern of alternative mRNA processing. Mol. Cell. Biol. **8:**186–195.
31. **Kerkhoff, E., K. Bister, and K. H. Klempnauer.** 1991. Sequence specific DNA binding by Myc proteins. Proc. Natl. Acad. Sci. USA **88:**4323–4327.
32. **Kohl, N., E. Leguoy, R. A. DePinho, P. Nisen, R. Smith, C. E. Gee, and F. W. Alt.** 1986. Human N-*myc* is closely related in organization and nucleotide sequence to c-*myc*. Nature (London) **319:**73–77.
33. **Kohl, N. E., N. Kanda, R. R. Schreck, G. Bruns, S. A. Latt, F. Gilbert, and F. W. Alt.** 1983. Transposition and amplification of oncogene-related sequences in human neuroblastomas. Cell **35:**359–367.
34. **Kretzner, L., W. M. Blackwood, and R. N. Eisenman.** 1992. *myc* and *max* proteins possess distinct transcriptional activities. Nature (London) **359:** 426–429.
35. **Land, H., L. F. Parada, and R. A. Weinberg.** 1983. Tumorigenic conversion of primary embryo fibroblasts requires at least two cooperating oncogenes. Nature (London) **304:**596–602.

35a. **Lee, H.-W., and R. A. DePinho.** Unpublished data.

36. **Leguoy, E., R. DePinho, K. Zimmerman, R. Collum, G. Yancopoulos, L. Mitsock, R. Kriz, and F. W. Alt.** 1987. Structure and expression of the murine L-*myc* gene. EMBO J. **11:**3359–3366.
37. **Lowry, O. H., J. J. Rosebrough, A. L. Farr, and R. J. Randall.** 1951. Protein measurement with the Folin phenol reagent. J. Biol. Chem. **193:**265–275.
38. **Luscher, B., and R. N. Eisenman.** 1990. New light on Myc and Myb. Part I. Myc. Genes Dev. **4:**2025–2035.
39. **Ma, A., T. Moroy, R. Collum, H. Weintraub, F. W. Alt, and K. Blackwell.** 1993. DNA binding by N- and L-*myc* proteins. Oncogene **8:**1093–1098.
40. **Mackem, S., and K. A. Mahon.** 1991. *Ghox 4.7*: a chick homeobox gene expressed primarily in limb buds with limb-type differences in expression. Development **112:**791–806.
41. **Mansour, S. L., K. R. Thomas, and M. R. Capecchi.** 1988. Disruption of the proto-oncogene int-2 in mouse embryo-derived stem cells: a general strategy for targeting mutations to non-selectable genes. Nature (London) **336:**348–352.
42. **Moens, C. B., A. B. Auerbach, R. A. Conlon, A. L. Joyner, and J. Rossant.** 1992. A targeted mutation reveals a role for N-*myc* in branching morphogenesis in the embryonic mouse lung. Genes Dev. **6:**691–704.
43. **Morgenbesser, S. D., and R. A. DePinho.** 1993. Use of transgenic mice to study Myc family gene function in normal mammalian development and in cancer. Semin. Cancer Biol. **5:**21–36.
44. **Morgenbesser, S. D., N. Schreiber-Agus, M. Bidder, K. A. Mahon, P. Overbeek, J. Horner, and R. A. DePinho.** 1995. Contrasting roles for c-Myc and L-myc in the regulation of cellular growth and differentiation *in vivo*. EMBO J. **14:**743–756.
45. **Moroy, T., P. Fisher, C. Guidos, A. Ma, K. Zimmerman, A. Tesfaye, R. A. DePinho, I. Weissman, and F. W. Alt.** 1990. IgH enhancer deregulated expression of L-*myc*: abnormal T-lymphocyte development and T-cell lymphomagenesis. EMBO J. **9:**3659–3666.
46. **Moroy, T., P. Fisher, G. Lee, T. Achacoso, F. Wiener, and F. W. Alt.** 1992. High frequency of myelomonocytic tumors in aging Eu L-*myc* transgenic mice. J. Exp. Med. **175:**313–322.
47. **Mugrauer, G., F. W. Alt, and P. Ekblom.** 1988. N-*myc* protooncogene expression during organogenesis in the developing mouse as revealed by in-situ hybridization. J. Cell Biol. **107:**1325–1335.
48. **Mugrauer, G., and P. Ekblom.** 1991. Contrasting expression patterns of three members of the Myc family of protooncogenes in the developing and adult mouse kidney. J. Cell Biol. **112:**13–25.
49. **Mukherjee, B., S. D. Morgenbesser, and R. A. DePinho.** 1992. Myc-family oncoproteins function through a common pathway to transform normal cells in culture: cross-interference by Max and trans-activating dominant mutants. Genes Dev. **6:**1480–1492.
50. **Nau, M., B. Brooks, J. Batey, E. Sausville, A. Gasdar, I. Kirsh, O. McBride, V. Bertness, G. Hollis, and J. Minna.** 1985. L-*myc*, a new *myc*-related gene amplified and expressed in human small cell lung carcinomas. Nature (London) **318:**69–73.
51. **Peterson, G. L.** 1993. Determination of total protein. Methods Enzymol. **91:**95–119.
52. **Prendergast, G. C., D. Lawe, and E. B. Ziff.** 1991. Association of *myn*, the murine homolog of *max*, with c-*myc* stimulates methylation sensitive DNA binding and *ras* cotransformation. Cell **65:**395–407.
53. **Prendergast, G. C., and E. B. Ziff.** 1991. Methylation-sensitive sequence-specific DNA binding by the c-*myc* basic region. Science **251:**186–189.
54. **Rapola, J., I. Jarvela, and L. Peltonen.** 1991. The neuronal ceroid lipofuscinoses: unfolding the genetic defect. Pediatr. Pathol. **11:**799–806.
55. **Robertson, E. J. (ed.).** 1987. Teratocarcinomas and embryonic stem cells: a practical approach, p. 71–112. IRL Press, Oxford.
56. **Rudnicki, M. A., T. Braun, S. Hinuma, and R. Jaenisch.** 1992. Inactivation of MyoD in mice leads to up-regulation of the myogenic HLH gene *Myf-5* and results in apparently normal muscle development. Cell **71:**383–390.
57. **Saga, Y., T. Yugi, Y. Ikawa, T. Sakakura, and S. Aizawa.** 1992. Mice develop normally without tenascin. Genes Dev. **6:**1821–1831.
58. **Sawai, S. A., K. Shimono, Y. Yakamatsu, C. Palmes, K. Hanaoka, and H. Kondoh.** 1993. Defects of embryonic organogenesis resulting from targeted disruption of the N-*myc* gene in the mouse. Development **117:**1445–1455.
59. **Schmid, P., W. A. Schulz, and H. Hameister.** 1989. Dynamic expression of the *myc* protooncogene in midgestation mouse embryos. Science **242:**226–229.
60. **Schreiber-Agus, N., J. Horner, R. Torres, F.-C. Chiu, and R. A. DePinho.** 1993. Zebra fish *myc* family and *max* genes: differential expression and oncogenic activity throughout vertebrate evolution. Mol. Cell. Biol. **13:**2765–2775.
61. **Schreiber-Agus, N., R. Torres, J. Horner, A. Lau, M. Jamrich, and R. A. DePinho.** 1993. Comparative analysis of the expression and oncogenic activities of *Xenopus* c-, N-, and L-*myc* homologs. Mol. Cell. Biol. **13:**2456–2468.
62. **Schwab, M., K. Alitalo, L. Klempnauer, H. Varmus, J. M. Bishop, F. Gilbert, G. Brodeur, M. Goldstein, and J. Trent.** 1983. Amplified DNA with limited homology to *myc* cellular oncogene is shared by human neuroblastoma cell lines and a neuroblastoma tumor. Nature (London) **305:**245–248.
63. **Schwab, M., H. E. Varmus, and J. M. Bishop.** 1985. The human N-*myc* gene contributes to tumorigenic conversion of mammalian cells in culture. Nature (London) **316:**160–162.
64. **Sheiness, D., and J. M. Bishop.** 1979. DNA and RNA from uninfected vertebrate cells contain nucleotide sequences related to the putative transforming gene of avian myelocytomatosis virus. J. Virol. **31:**514–521.
65. **Sheiness, D., S. H. Hughes, H. E. Varmus, E. Stubblefield, and J. M. Bishop.** 1980. The vertebrate homolog of the putative transforming gene of avian myelocytomatosis virus: characteristics of the DNA locus and its RNA transcript. Virology **105:**415–424.
66. **Stanton, B. R., A. Perkins, L. Tessarollo, D. Sassoon, and L. Parada.** 1992. Loss of N-Myc function results in embryonic lethality and failure of the epithelial component of the embryo to develop. Genes Dev. **6:**2235–2247.
67. **Stanton, L. W., P. D. Fahrlander, P. M. Tesser, and K. B. Marcu.** 1986. Nucleotide sequence comparison of normal and translocated murine c-*myc* genes. Nature (London) **310:**423–425.
68. **Torres, R., N. Schreiber-Agus, S. D. Morgenbesser, and R. A. DePinho.** 1992. Myc and Max: a putative transcriptional complex in search of a cellular target. Curr. Opin. Cell Biol. **4:**468–474.
69. **Tso, J. Y., X. H. Sun, T. H. Kao, K. S. Reece, and R. Wu.** 1985. Isolation and characterization of rat and human glyceraldehyde-3-phosphate dehydrogenase cDNA; genomic complexity and molecular evolution of the gene. Nucleic Acids Res. **13:**2485–2502.
70. **Vesa, J., E. Hellsten, L. Verkruyse, L. Camp, J. Rapola, P. Santavuori, S. Hofman, and L. Peltonen.** 1995. Mutations in the palmitoyl protein thioesterase gene causing infantile neuronal ceroid lipofuscinosis. Nature (London) **376:**584–587.
71. **Wenzel, A., C. Cziepluch, U. Hamann, J. Schurmann, and M. Schwab.** 1991. The N-*myc* oncoprotein is associated *in vivo* with the phosphoprotein Max (p20/p22) in human neuroblastoma cells. EMBO J. **10:**3703–3712.
72. **Xu, L., R. Wallen, V. Patel, and R. A. DePinho.** 1993. Role of first exon/intron sequences in the regulation of Myc family oncogenic potency. Oncogene **8:**2547–2554.
73. **Yancopoulos, G. D., P. Nisen, A. Tesfaye, N. E. Kohl, M. Goldfarb, and F. W. Alt.** 1985. N-Myc can cooperate with Ras to transform normal cells in culture. Proc. Natl. Acad. Sci. USA **82:**5455–5459.
74. **Zimmerman, K. A., G. D. Yancopoulos, R. G. Collum, R. K. Smith, N. E. Kohl, K. A. Denis, M. M. Nau, O. N. Witte, D. Toran-Allerand, C. E. Gee, and F. W. Alt.** 1986. Differential expression of *myc* family genes during murine development. Nature (London) **319:**780–783.